Journal of Electronics and Electrical Engineering
https://ojs.wiserpub.com/index.php/JEEE

Research Article

A Stochastic Geometry Analysis on The Uplink Performance of Cell-Free Massive MIMO Systems with Hardware Impairments

Emmanuel Ampoma Affum[1,*], Edward Danso Ansong [2], Kwame Oteng Gyasi [1], Maxwell Afriyie Oppong[3], Isaac Kweku Boakye[4], Francois Sekyere[5], Louis Owusu Annan[6]

[1] Department of Telecommunication Engineering, Kwame Nkrumah University of Science and Technology, Kumasi-Ghana.
[2] Department of Computer Science, School of Mathematical Science, University of Ghana, Accra-Ghana.
[3] Department of Electrical and Electronic Engineering, Kumasi Technical University, Kumasi-Ghana.
[4] Civil Aviation Authority, KIA-Airport, Accra-Ghana.
[5] Electrical Department, Akenten Appiah-Menka University of Skills Training and Entrepreneurial Development
[6] Technical and Services, Anwomaso Thermal Power Station, Volta River Authority, Kumasi-Ghana.
E-mail: ampoma.uestc@yahoo.com

Received: 6 May 2025; **Revised:** 23 June 2025; **Accepted:** 15 August 2025

Abstract: Numerous studies have demonstrated that the benefits of Cell-Free Massive Multiple-Input-Multiple-Output (CF-mMIMO), including consistent coverage, increased Spectral Efficiency (SE), and improved security, cannot be overstated. CF-mMIMO employs distributed Access Points (APs) to eliminate inter-cell interference, a major limitation in traditional cell-based systems. CF-mMIMO relies mainly on low-grade and low-cost hardware transceiver elements, User Equipment (UE), and Internet of Things (IoT) devices to reduce costs. This introduces Hardware Imperfections (HWI) that may degrade network performance, and their impact on system performance requires extensive research. Most current research assumes incorrectly that transceiver hardware is perfect in real-world deployments where low-cost or energy-constrained devices are used. However, HWI, due to low-grade and low-cost elements, produces distortion noise and hinders system performance, especially in the uplink. Moreover, most investigations analyzing the impact of HWI consider the correlation-based Rayleigh model, instead of the geometry-based model that factors practical parameters such as path loss, delay profile, and Angle of Arrival. Another challenge is that the spatial randomization of user and AP sites complicates the impact of HWI. The idea of a spatial channel has surprisingly not been integrated into the HWI analysis in previous publications. Our stochastic-geometry uplink analysis of the CF-mMIMO system includes these and many more reasons. We model the location of APs with a Poisson Point Process (PPP) instead of a uniform distribution. We considered the AP as a ULA and integrated its array response into the channel vector to achieve spatial surroundings for evaluation. The proposed CF-mMIMO model was evaluated using different combining schemes, including Minimum Mean Square Error (MMSE), Regularized Zero-Forcing (RZF), and Maximum Ratio (MR). Monte Carlo simulations reveal that hardware-induced distortions significantly degrade CF-mMIMO's performance. The outcome indicates that in a stochastic channel, the rate of degradation for both RZF and MMSE is the same, although MMSE occasionally outperforms RZF by a small margin. Furthermore, MR has a lower overall efficiency, even though it can be more resilient. Finally, increasing the number of Uniform Linear Array (ULA) elements was expected to improve SE, as reported by prior research. The stochastic channel with ULA marginally outperformed the correlated Rayleigh model due to spatial environment effects. An ideal (non-spatial) scenario confirmed this, showing a 55.62 percentage increment in SE.

Copyright ©2025 Emmanuel Ampoma Affum, et al.
DOI: https://doi.org/10.37256/jeee.4220257189
This is an open-access article distributed under a CC BY license
(Creative Commons Attribution 4.0 International License)
https://creativecommons.org/licenses/by/4.0/

Keywords: Hardware Impairment (HWI), Cell-Free Massive MIMO (CF-mMIMO), Spectral Efficiency (SE), Distortion Noise, Minimum Mean Square Error (MMSE), Regularized Zero-Forcing (RZF), Maximum Ratio (MR), Channel Estimation

1. Introduction

5G is a prominent wireless mobile communication network, employing various technologies including the Cell-Free Massive Multiple-Input-Multiple-Output (MIMO) system [1]. The traditional Multiple-Input-Multiple-Output (MIMO) system seeks to improve throughput and Spectral Efficiency (SE) by using multiple antennas at both the transmitter and receiver whilst serving many users simultaneously by deploying these Base Stations (BS) at various locations where each BS serves a particular geographical area called a cell as shown in Figure 1a.

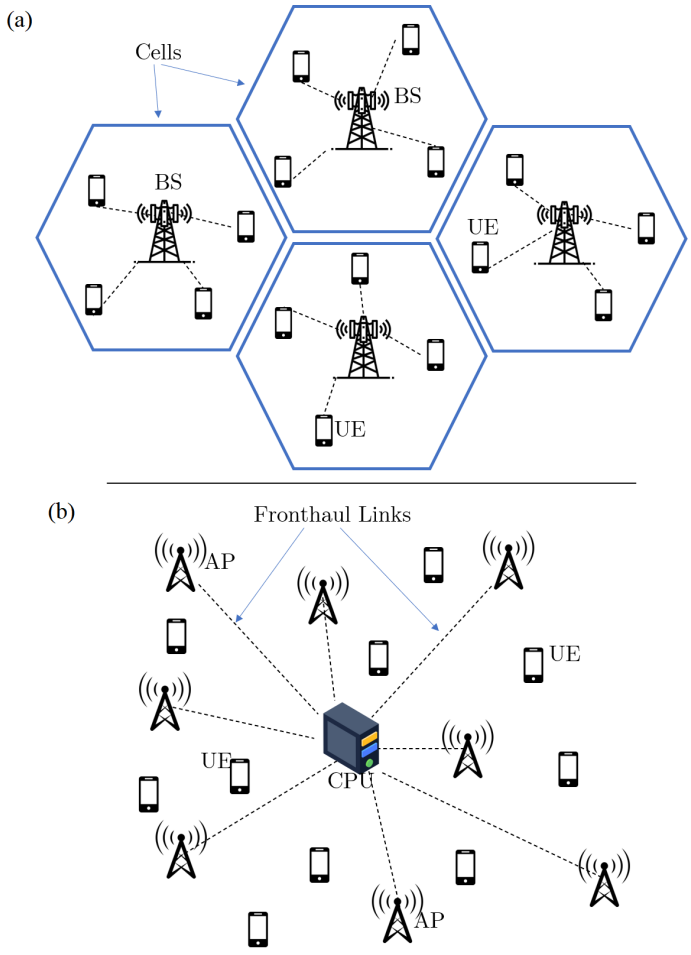

Figure 1. (a) Cellular MIMO, (b) Cell-Free MIMO

The limitations of this architecture stem mainly from the boundary between such cells, where users at these sites receive minimal power compared to those close to the BS. Another problem observed is that users at these sites experience inter-cell interference since they are also able to easily receive signals from neighboring cells. The Cell-Free architecture was mainly introduced to minimize these problems as much as possible. In the CF-mMIMO system as shown in Figure 1b, APs are strategically distributed across the coverage area, all access points connect to a CPU for coordination and have

multiple antennas to deliver optimal connection for all users. This effectively eliminates cell boundaries and allows the 5G system to support a wide range of edge devices, from smart homes to automated vehicles. This is a major requirement and key performance indicator for 5G [2, 3]. CF-mMIMO presents several key advantages. Its distributed antenna system significantly improves spatial diversity, reducing the effects of path loss and fading to deliver consistent quality of service across the coverage area.

Eliminating cells and utilizing centralized processing reduces inter-cell interference, leading to better signal quality and SE. Finally, CF-mMIMO allows for dynamic resource allocation, with the Central Processing Unit (CPU) optimizing power levels, beamforming weights, and user associations to enhance overall network performance. A major limiting factor in such systems is HWIs due to low-grade, low-cost elements that reduce system performance. These include amplifier non-linearity, phase noise, and IQ imbalance, all of which distort communication signals. HWIs are present in both base stations and User Equipment (UE); however, SE is dominated by hardware distortion at the UE [4], which shows that these HWIs have a greater impact when present on the user side than at the BS/AP in uplink scenarios. For manufacturers of end devices, the challenge is to balance cost-efficiency with performance, requiring the use of affordable transceiver hardware. However, such low-cost hardware often introduces impairments that distort signals and add to the performance issues already caused by the large number of MIMO transceiver elements.

1.1 *Review of existing works*

The impact of HWI on CF-mMIMO has been widely investigated to the level that algorithms to compensate for hardware impairments (HWIs) have been developed, but they cannot be fully dealt with [5]. Ref [6] studies the impact of these residual effects of impairments on the MIMO system. It was shown in [7] that impairments from the UE, rather than the BS as one might expect, limit the achievable SE, and that increasing the number of transmitting and receiving antennas simultaneously makes this limitation less severe. In [8], a model to quantify the compounded effect of individual HWIs is derived and analyzed, but only for the base station side. On the same subject, [9] shows that the distortion caused by HWIs at the BS can be treated as uncorrelated as the number of users increases, implying that the overestimation of the SE as the number of UEs increases becomes negligible. Note that all the papers mentioned above only performed analysis using the traditional cell-based MIMO approach. Using different levels of receive cooperation, [10] showed that SE performance improves with increased hardware quality. They also confirm that for the uplink, the HWI from the transmitter has a larger impact on the SE performance than that of the receiver.

By considering a limited capacity fronthaul link between APs and CPU, [11] presents transmission strategies in the presence of HWIs, but no specific categorization of how the HWI affected the transmission was made. Refs [12–14] in the analysis of scalable CF-mMIMO systems using different receivers show that additive HWIs becomes negligible as the number of AP antennas increases and that Partial MMSE combining has benefits over full MMSE combining even in the presence of HWIs. It is shown in [15–18] that low-resolution Analog-to-Digital Converters (ADC) which can be seen as the effect of imperfect hardware presents challenges even in the channel estimation stage and that user rate limits are mainly a results of low-resolution ADCs from user equipment. Non-ideal hardware was also found to significantly reduce channel estimation accuracy in [19], where the impact of phase drifts in different local oscillator setups was investigated. Again, the normalized mean square error for channel estimation increases as more HWI is presented into the system, as seen in [20]. Refs [4, 21] also determined that increasing the number of access points significantly mitigates the effects of only AP-side HWIs. Ref [22] shows that the location of these APs shouldn't be treated as uniformly distributed in the geographical space. In an attempt to compare performance between superimposed low-powered pilots and regular pilots, it was shown in [23] that the optimal power balance between pilot and data transmit powers that maximize SE is sensitive to only UE HWIs. At this point, it is worth highlighting that most works previously mentioned treated HWIs from both UEs and APs/BSs jointly without focusing specifically on UE HWIs.

Further research shows the impact of HWIs on the security of the network (secrecy performance) and achievable Energy Efficiency (EE). For instance, [24] shows that the impact of HWIs on energy efficiency becomes more noticeable as the severity increases. This is again seen in [25] where it was shown that for acceptable levels of HWIs, there was no detrimental influence on EE, especially for networks intended for high EE. Regarding secrecy performance, surprisingly, it was determined that additive distortion noise was advantageous to secrecy performance. All other forms of impairment

negatively affected secrecy performance, as shown in [26]. A proposed power allocation scheme is provided in [27] to improve secrecy performance reduction due to HWIs. Finally, a more recent study [28] investigated the effects of UE HWIs on the uplink using MMSE receive combining; it was found that better hardware quality improved the maximum achievable SE. A proposed solution to mitigate the effects of general HWIs is through the use of Reflective Intelligent Surface [29]. Table 1 summarizes recent related work on the impact HWI on the performance of MIMO systems.

Table 1. Summary of Related Work on HWI in CF-mMIMO systems

Ref	MIMO Type	Channel Model	Performance Metrics	Contribution
[4]	Cell-Free MIMO	Uncorrelated Rayleigh	Average SE	Proposed closed-form expressions for SE for both downlink and uplink under HWI which is used to create a new max-min power control algorithm for a fair and efficient system.
[8]	Cellular MU-MIMO	Frequency-Selective	Power Spectral Density, BER	Derived an aggregate statistical hardware impairment model to analyze distortion from HWI.
[9]	Cellular MIMO	i.i.d Rayleigh	Distortion-Over-Noise, Per-user SE	Produced a new receive combining scheme to maximize the SE, also compared SE under both correlated and uncorrelated distortion.
[10]	Cell-Free MIMO	i.i.d Rayleigh	Average SE, Sum SE	Investigated the SE performance under different receive cooperation levels, including Large Scale Fading Decoding and Simple Centralized Decoding.
[12]	Cell-Free MIMO	Correlated Rayleigh	Per-user SE	Developed a new expression to quantify the average achievable Spectral Efficiency (SE) with MMSE combining under the presence of HWIs.
[14]	User Centric CF-MIMO	Joint-Correlated Rayleigh	Per-user SE, Sum SE	Studied different receive combining schemes for scalable MIMO systems under HWI.
[17]	Cell-Free MIMO	Uncorrelated Rayleigh	NMSE, Sum SE	It was found that APs can tolerate lower quality hardware as the number of total APs increase.
[19]	Cell-Free MIMO	Uncorrelated Rayleigh	NMSE, Sum SE	By employing the LMMSE channel estimator, exact uplink closed-form achievable rate expressions with MRC receiver filters for both Common and Separate Local Oscillator setups were derived.
[22]	Cell-Free MIMO	Correlated Rayleigh	Coverage Probability, Achievable Rate	Taking into consideration the random position of APs in the cell-free network using stochastic geometry, the downlink performance was investigated
[21]	Cell-Free MIMO	Uncorrelated Rayleigh	Average SE	A closed form expression for uplink SE that reveals how HWI at the UEs and APs affect SE and it was proven that the impact of the AP hardware quality becomes very much negligible as the number of APs increase.
[28]	Cell-Free MIMO	Correlated Rayleigh	Per-user SE, Sum SE	Closed-form expression for channel estimation under HWI is derived with the MMSE estimator and investigations on SE were made using different combining schemes.

1.2 *Motivation and contribution*

The literature mentioned above makes it abundantly evident that the advantages of CF-mMIMO delivery of high data rates cannot be overstated. However, in real-world deployments when low-cost or energy-constrained devices are utilized, the majority of current research makes the erroneous assumption that transceiver hardware is perfect. Phase noise, amplifier non-linearities, and I/Q imbalance are examples of HWIs that produce distortion noise and hinder system performance, especially in the uplink. Additionally, the majority of studies examining the effects of HWI use the correlation-based Rayleigh model rather than the geometry-based model that takes into account realistic parameters like path loss, delay profile, and angle of arrival. Furthermore, one challenge is that the spatial randomization of user and AP sites is another issue that makes the effects of HWI more complicated. Surprisingly, prior studies have largely overlooked the concept of spatial channels in HWI analysis. To reduce that gap and facilitate more informed system design and deployment methods, this research analyzes SE under hardware limitations. We incorporate the array response of ULA to display the spatial surrounds and determine the whole impact of UE HWI on the network. Moreover, there have not been much research done on how well CF-mMIMO performs when combined with HWI in a stochastic channel model. Although the stochastic channel has superior channel properties, the frequently used correlated Rayleigh channel does not. The performance of combining schemes in a CF-mMIMO stochastic channel is essential for a comprehensive analysis of CF-mMIMO.

Additionally, prior research has shown that the correlated Rayleigh channel achieves the best performance with the MMSE combining strategy. To validate current literature, the question here is whether the MMSE will perform similarly in the stochastic channel. When comparing a correlated channel to a stochastic channel, will the MMSE provide the same rate of degradation?

In this research, we particularly study the compounded effects of UE HWIs on the uplink SE of the CF-mMIMO network. Moreover, we analyze the uplink using a Stochastic Geometry approach since in that case the UE is the originator of the signal, and that will serve well for effective investigation. Using the suggested stochastic model, the probability distribution of SE across various combining approaches was first examined using RZF, MR, and MMSE. The CDF at a specific SE value in the study indicates the likelihood that the SE is less than or equal to that value. According to our analysis, a steeper curve indicates that the SE is concentrated within a particular range, whereas a gradual increase indicates greater SE variability. The practical consequences include helping to choose the optimal combining technique based on the distribution of SE, offering insight into how diversity strategies operate in different channel conditions, and, lastly, helping to design and optimize communication systems. The Average Sum Spectral Efficiency (SE) at various HWI levels for various receiver combining schemes was examined to verify the effectiveness of combining schemes utilizing the stochastic model with HWI. This is to ascertain how SE is affected by UE hardware imperfections. Lastly, we assess the performance loss resulting from impairments, the Average Sum Spectral Efficiency vs Number of User Equipments for various combining schemes, with and without HWIs, was investigated.

The main contributions of this paper can be summarized as follows:

• We present an uplink system model of a stochastic CF-mMIMO considering UE HWIs. This involves providing a mathematical model to represent the compounded UE HWI, path loss, delay profile, and angle of arrival. To show the spatial surroundings and ascertain the complete effect of UE HWI on the network, we integrate the array response of ULA in the channel model.

• We use various combining schemes, such as MR, RZF, and MMSE, to analyze the SE performance. This is to find out if the impact of UE HWI in the stochastic channel caused by these combining strategies would result in the same performance loss as the current fact in a correlated channel.

• We present results to demonstrate that in a stochastic CF-mMIMO system, MMSE and RZF are preferable as they provide superior SE, particularly when managing several users. Although there are times when MMSE performs slightly better than RZF, the rate of degradation for both schemes in a stochastic channel is the same. Our results confirm that MR performs the weakest of the three and is hence more susceptible to HWIs. Furthermore, although MR may be more robust, it comes at the expense of poorer overall efficiency. Therefore, additional processing techniques (such as MMSE) are necessary to maintain acceptable performance for a cell-free stochastic mMIMO with considerable HWIs. Interestingly, it was expected that as the number of antenna elements increased, the ULA would enhance the SE performance, supporting the corpus of existing literature. However, the performance of the stochastic channel with ULA was slightly better than that of the correlated Rayleigh channel. This is due to the addition of spatial surroundings to the channel vector. We verify this by considering the unrealistic case of generating the channel vector in an ideal situation (i.e., without a spatial environment). The SE rose by 55.62% as a result. Therefore, it is clear that the spatial context is an important component of CF-mMIMO that channel modeling engineers cannot undervalue.

1.3 *Paper organization*

The remainder of this paper is organized in the following manner. Section 2 presents the network and signal modeling with impairments. Section 3 brings about an analysis used to compute SE. Section 4 reveals numeric results and Section 5. concludes the paper based on observations made.

Notation: Uppercase boldface letters, $\mathbf{X}$, denote matrices, lowercase boldface letters, $\mathbf{x}$, denote column vectors. Sets are represented by calligraphic letters $\mathscr{X}$. The superscripts ^{T}, *, ^{H} represents transpose, conjugate and conjugate transpose respectively. $\mathbb{C}^{x\times y}$ represents the set of $x \times y$ complex-valued matrices. $\mathscr{N}_{\mathbb{C}}(0,\mathbf{R})$ denotes a circularly symmetric complex Gaussian distribution with zero mean and correlation matrix $\mathbf{R}$. $\delta()$ represents the Dirac Delta function and lastly, $\mathbb{E}\{x\}$ represents the expected value of x.

2. Cell-Free system model for angle of arrival and spatial channel

Consider a fully centralized processing CF-mMIMO network with K single antenna UEs, M number of APs with each having N number of antennas and L_{mk} number of multipath components from AP m to user k, all APs connect to the CPU for centralized processing via fronthaul, as described in Figure 2. The AP locations $\{x_i\} \subset \mathbb{R}^2$ are generated randomly and follow a two-dimensional homogeneous Poisson Point Process (PPP) Φ_{AP} with density λ_{AP} [APs/km^2]. Let the finite-sized geographic area denoted by $\mathscr{A}$ occupy space $S(\mathscr{A})$ m^2. In a specific realization of the PPP Φ_{AP}, the number of APs M is a random variable following the Poisson distribution with mean $\tilde{M} = \mathbb{E}[M]$ given by

$$\tilde{M} = \lambda_{AP} S(\mathscr{A}) \tag{1}$$

The total number of antennas in $\mathscr{A}$ is a Poisson random variable denoted by $\mathscr{W} = MN$ with mean $\mathbb{E}[\mathscr{W}] = \tilde{M}N$ and the assumption is that $\mathscr{W} >> K$ corresponding to a CF-mMIMO scenario.

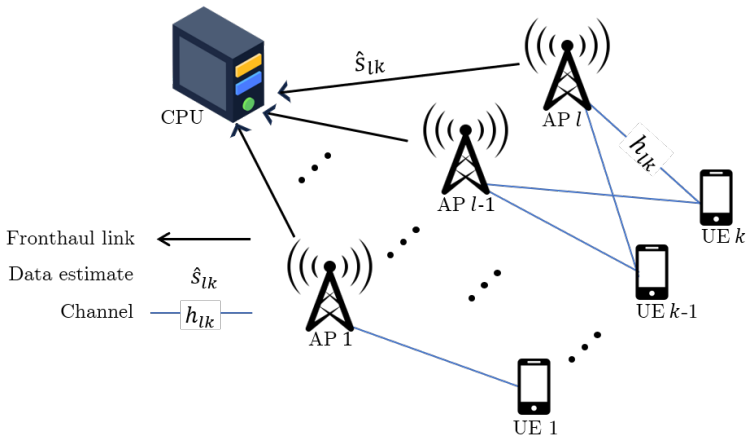

Figure 2. Cell-Free MIMO setup with centralized processing

The channel vector $\mathbf{h}_{mk}(t)$ between any UE k and AP l is defined as:

$$\mathbf{h}_{mk}(t) = \sum_{l=1}^{L_{mk}} \sqrt{\beta_{mkl}} \mathbf{a}_m(\theta_{mkl}) e^{j\phi_{mkl}} \delta(t - \tau_{mkl}) \tag{2}$$

where $\phi_{mkl} \sim (0, 2\pi)$ is the random phase, $\mathbf{a}_m(\theta_{mkl}) = \frac{1}{N}[1, e^{j\frac{2\pi d}{\lambda} sin(\theta)}, \ldots, e^{j\frac{2\pi d}{\lambda}(N-1)\sin(\theta)}]^T$ describes the array response vector of AP m at θ_{mkl} Angle of Arrival (AoA) with carrier frequency of λ. $\tau_{mkl} = \frac{d_{mkl}}{c}$, with c being the speed of light and d_{mkl} being the physical path, describes the delay of the lth path and β_{mkl} represents the power of the lth path which accounts for path loss and delay profile and is given by:

$$\beta_{mkl} = G_0 (\frac{d_{mkl}}{d_0})^{-\gamma} 10^{\frac{\sigma_{mkl}}{10}} \tag{3}$$

where G_0 is the reference gain at distance d_0, d_{mkl} is the distance between AP m and user k via the lth path, γ is the path loss exponent and $\sigma_{mkl} \sim \mathcal{N}(0, \sigma^2_{shadow})$ represents log-normal shadowing.

The uplink being investigated consists of a τ_c coherence blocks where τ_p channels are reserved for pilot transmission and $(\tau_c - \tau_p)$ channels are used for data transmission as illustrated in Figure 3.

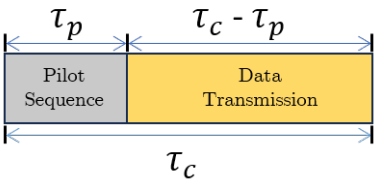

Figure 3. Uplink massive MIMO coherence block channel

The distortion due to HWI can be modeled by:

$$\eta_t \sim \mathcal{N}_{\mathbb{C}}(0, \kappa_t^2 \rho_i), \quad \eta_r \sim \mathcal{N}_{\mathbb{C}}(0, \kappa_r^2 \rho_i |\mathbf{h}|^2) \tag{4}$$

where $\kappa_t^2, \kappa_r^2 \geq 0$ represent design parameters that characterize the HWI levels at the transmitter and receiver respectively, and η_t is the transmitter distortion, our focus in this project.

Since we only look at HWI from the UE in the uplink case, we will stress only on κ_t and ignore κ_r for investigation purposes. The received signal by AP l from UE k is given by:

$$\mathbf{y}_m = \sum_{k=1}^{K} l_{mk}^{1/2} \mathbf{g}_{mk} (\sqrt{p} s_k + \eta_t) + \mathbf{n}_m \tag{5}$$

since κ_r is assumed non-existent then the power of the compounded distortion at the receiver for any given channel realization in [30] (4) reduces to:

$$\mathbb{E}_{\eta_t, \eta_r} \{ |\mathbf{h}_t \eta_t + \eta_r|^2 \} = \rho_i |\mathbf{h}_t|^2 \kappa_t^2 \tag{6}$$

Hence forth we will represent the overall HWI level by $\kappa = \kappa_t$ and the overall distortion by $\eta = \eta_t$.

2.1 *Channel estimation*

Knowledge about the channel between any AP and UE is crucial during data signal recovery as it allows the AP to filter out the desired signal and suppress channel noise and interference from other UEs. In order to estimate $\mathbf{h}_{mk}$ using the MMSE estimator, τ_p mutually orthogonal pilot sequences are transmitted to the APs by each UE, $\psi_{mk} \in \mathbb{C}^{\tau_p}$ represents the pilot sequence from UE k to AP l such that $||\psi_{mk}||^2 = 1$. The received signal $\mathbf{Y}_m^p \in \mathbb{C}^{N \times \tau_p}$ at AP l is given by :

$$\mathbf{Y}_m^p = \sum_{k=1}^{K} l_{mk}^{1/2} \mathbf{g}_{mk} (\sqrt{\tau_p \rho_k} \psi_{mk}^T + \eta) + \mathbf{N}_l \tag{7}$$

where ρ_k is the normalized signal-to-noise ratio, and $\mathbf{N}_l \in \mathbb{C}^{N \times \tau_p}$ represents the additive receiver noise.Channel estimation at AP l is performed by projecting $\mathbf{Y}_m^p$ onto $\frac{1}{\sqrt{\tau_p \rho_k}} \psi_k$ to obtain:

$$\frac{1}{\sqrt{\tau_p \rho_k}} \mathbf{Y}^p_{mk} \psi_k = \mathbf{y}^p_{mk} = \frac{1}{\sqrt{\tau_p \rho_k}} \sum_{k=1}^{K} l_{mk}^{1/2} \mathbf{g}_{mk} (\sqrt{\tau_p \rho_k} \psi_{mk} + \eta) \psi_{mk} + \frac{1}{\sqrt{\tau_p \rho_k}} \mathbf{N}_l \psi_{mk} \tag{8}$$

which can be expanded as:

$$\begin{aligned} \mathbf{y}^p_{mk} = & \underbrace{\mathbf{g}_{mk} l_{mk}^{1/2}}_{\text{Desired Pilot}} + \underbrace{\sum_{i=1, i \neq k}^{K} l_{mk}^{1/2} \mathbf{g}_{mk} \psi^H_{mk} \psi_{mk}}_{\text{Interference}} + \underbrace{\sum_{i=1}^{K} \frac{1}{\sqrt{\tau_p \rho_k}} l_{mk}^{1/2} \mathbf{g}_{mk} \eta \psi_{mk}}_{\text{Hardware Distortion}} \\ & + \underbrace{\frac{1}{\sqrt{\tau_p \rho_k}} \mathbf{N}_l \psi_{mk}}_{\text{Noise}} \end{aligned} \tag{9}$$

By applying standard results as in [22], the processed signal in (9) can now be used to compute the MMSE channel estimate $\hat{\mathbf{h}}_{mk} \sim \mathcal{N}_{\mathbb{C}}(0, \sigma^2 \mathbf{I}_N)$ shown as:

$$\begin{aligned} \hat{\mathbf{h}_{mk}} &= \mathbb{E}\{\mathbf{h}^H_{mk} \mathbf{y}_{mk}\} (\mathbb{E}\{\mathbf{y}_{mk} \mathbf{y}^H_{mk}\})^{-1} \mathbf{y}_{mk} \\ &= \frac{l_{mk}}{\sum_{i=1}^{K} (|\psi^H_{mk} \psi_{mk}|^2 l_{mi} + \kappa^2 \rho_k l_{mi}) + \frac{1}{\tau_p \rho_k}} \mathbf{y}_{mk} \end{aligned} \tag{10}$$

The aim is to make the error in estimation $\tilde{\mathbf{h}}_{mk} = \mathbf{h}_{mk} - \hat{\mathbf{h}}_{mk}$ as minimal as possible with distribution $\tilde{\mathbf{h}}_{mk} \sim \mathcal{N}_{\mathbb{C}}(0, \tilde{\sigma}^2 \mathbf{I}_N)$. Additionally we denote the vectors $\mathbf{h}_k = [\mathbf{h}^T_1 \cdots \mathbf{h}^T_{M_k}]^\top \in \mathbb{C}^{W \times 1} \sim \mathcal{N}_{\mathbb{C}}(0, \mathbf{L}_k)$, $\hat{\mathbf{h}}_k = [\hat{\mathbf{h}}^T_{1k} \cdots \hat{\mathbf{h}}^T_{M_k}]^\top \in \mathbb{C}^{W \times 1} \sim \mathcal{N}_{\mathbb{C}}(0, \Phi_k)$ and $\tilde{\mathbf{h}}_k \in \mathbb{C}^{W \times 1} \sim \mathcal{N}_{\mathbb{C}}(0, \mathbf{C}_k = \mathbf{L}_k - \Phi_k)$, where the matrices $\mathbf{L}_k$, $\Phi_k = \mathbf{L}^2_k \mathbf{D}^{-1}$, and $\mathbf{D}$ are $W \times W$ are block diagonal, i.e., $\mathbf{L}_k = \text{diag}\,(l_{1k} \mathbf{I}_N, \ldots, l_{Mk} \mathbf{I}_N)$, $\Phi_k = \text{diag}\left(\sigma^2_{1k} \mathbf{I}_N, \ldots, \sigma^2_{Mk} \mathbf{I}_N\right)$, and $\mathbf{D} = \text{diag}\,(d_1 \mathbf{I}_N, \ldots, d_M \mathbf{I}_N)$, respectively.

2.2 *Uplink data transmission*

Data symbols are sent from the UEs to the APs. The received signal at each AP l is then given as:

$$\mathbf{y}_l = \sum_{i=1}^{K} \mathbf{h}_{mi} (s_i + \eta) + \mathbf{n_l} \tag{11}$$

The CPU obtains an estimate $\hat{s}_k$ of the transmitted signal s_k by linearly combining the individual local estimates received from all APs. Each local estimate corresponds to an inner product between the received signal $\mathbf{y}_l$ at AP l and its corresponding combining vector $\mathbf{v}_{mk}$.

$$\hat{s}_k = \underbrace{\mathbf{v}_k^H \hat{\mathbf{h}}_k s_k}_{\text{Desired signal over estimated channel}} + \underbrace{\mathbf{v}_k^H \tilde{\mathbf{h}}_k s_k}_{\text{Desired signal over unknown channel}} + \underbrace{\sum_{i=1, i\neq k} \mathbf{v}_k^H \mathbf{h}_i s_i}_{\text{Interference}} + \underbrace{\sum_{i=1,} \mathbf{v}_k^H \mathbf{h}_i \eta}_{\text{Hardware distortion}} + \underbrace{\mathbf{v}_k^H \mathbf{n}}_{\text{Noise}} \tag{12}$$

The estimate at the CPU is expressed in (12) and can be broken down into the following components:

• Desired Signal over Estimated Channel ($\mathbf{v}_k^H \hat{\mathbf{h}}_k s_k$):

This term represents the contribution of the desired signal that passes through the *estimated* channel $\hat{\mathbf{h}}_k$. It is the useful part of the signal that the system aims to recover.

• Desired Signal over Unknown Channel ($\mathbf{v}_k^H \tilde{\mathbf{h}}_k s_k$):

This term accounts for the portion of the desired signal that is affected by *channel estimation errors* $\tilde{\mathbf{h}}_k$, introducing self-interference during signal recovery.

• Interference ($\sum_{i=1, i\neq k} \mathbf{v}_k^H \mathbf{h}_i s_i$):

This represents *inter-user interference* caused by simultaneous transmissions from other users ($i \neq k$), whose signals are received through their respective channels $\mathbf{h}_i$.

• Hardware Distortion ($\sum_{i=1} \mathbf{v}_k^H \mathbf{h}_i \eta$):

This term captures distortions resulting from *HWIs* at both the transmitters and receivers, modeled by η. These impairments affect all incoming signals.

• Noise ($\mathbf{v}_k^H \mathbf{n}$):

This term represents the contribution of *additive noise* $\mathbf{n}$ at the receivers, filtered by the combining vector. It models the random thermal noise inherent in all practical systems.

3. Uplink Spectral Efficiency analysis

To assess the best achievable output SE for the network the first term in (12) is treated as the desired signal part and the other 4 terms are treated as noise and interference. The uplink ergodic capacity of UE k is lower bounded by:

$$\mathbf{c} \geq \mathbf{SE}_k = \frac{\tau_u}{\tau_c} \mathbb{E}\{\log_2(1 + \mathbf{SINR}_k)\} \tag{13}$$

and

$$\mathbf{SINR}_k = \frac{\rho_k |\mathbf{v}_k^H \hat{\mathbf{h}}_k|^2}{\mathbf{v}_k^H (\sum_{i=1}^K \rho_i (\hat{\mathbf{h}}_i \hat{\mathbf{h}}_i^H + \mathbf{C}_i) + \mathbf{Z}_k) \mathbf{v}_k} \tag{14}$$

where

$$\mathbf{Z}_k = (1 - \kappa^2) \rho_i \hat{\mathbf{h}}_k \hat{\mathbf{h}}_k^H + \sigma^2 \mathbf{I}_N \tag{15}$$

The following combining schemes are presented by the authors in [28] to compare network performance under UE HWI using different combining schemes at the receiver. These are used to combine the desired signal and simultaneously improve the Signal-to-Interference-plus-Noise Ratio (SINR) using channel information obtained.

• MMSE

The MMSE combining has been shown to maximize the SINR in (14). The combining vector is given by:

$$\mathbf{v}_k^{MMSE} = (\sum_{i=1}^{K} \rho_i(\hat{\mathbf{h}}_i\hat{\mathbf{h}}_i^H + \mathbf{C}_i) + \sigma^2\mathbf{I}_N)^{-1}\hat{\mathbf{h}}_k \tag{16}$$

Although this may provide the best results, especially in noisy environments, it has very high computational complexity due to the matrix operations involved.

• RZF

This scheme provides the best trade-off between computational needs and SINR by ignoring all error estimation correlation matrices in (16) and suppresses noise during combining effectively. This is given by:

$$\mathbf{v}_k^{RZF} = (\sum_{i=1}^{K} \rho_i\hat{\mathbf{h}}_i\hat{\mathbf{h}}_i^H + \sigma^2\mathbf{I}_N)^{-1}\hat{\mathbf{h}}_k \tag{17}$$

• MR

The combining vector is simply given by $\mathbf{v}_k^{MR} = \hat{\mathbf{h}}_k$ and has the highest computational efficiency but becomes more susceptible to noise as the number of users grow large.

4. Numerical results and discussion

Using Monte-Carlo simulations, the analysis started by generating the CF-mMIMO channel vector in equation (2) using the delay profile in (3), the array response of ULA, the delay spread, and the path loss. Equation (10), after SE evaluation at different HWI levels using MMSE, RZF, and MR using equations (15), (16), and (17), respectively, was used to estimate the channel. Table 2 provides the relevant simulation parameters.

Table 2. Simulation parameters for stochastic geometry channels

Parameter Name	Notation	Value
Number of Users	K	40
Number of Antennas	N	4
Coherence Block	τ_c	200
Pilot Sequences	τ_p	10
Transmission Power (mW)	p	100
Bandwidth (MHz)	B	20
Noise Variance (dBm)	σ^2	-96

Figure 4 illustrates the Cumulative Distribution Function (CDF) of the uplink Spectral Efficiency for MMSE, RZF, and MR combining schemes under the stochastic geometry-based channel. The CDF at a given SE value indicates the probability that the SE is less than or equal to that value.

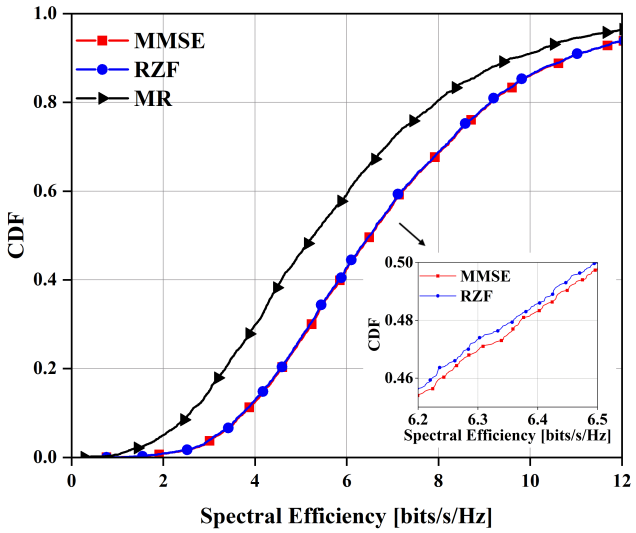

Figure 4. The uplink SE comparison for the different combining schemes

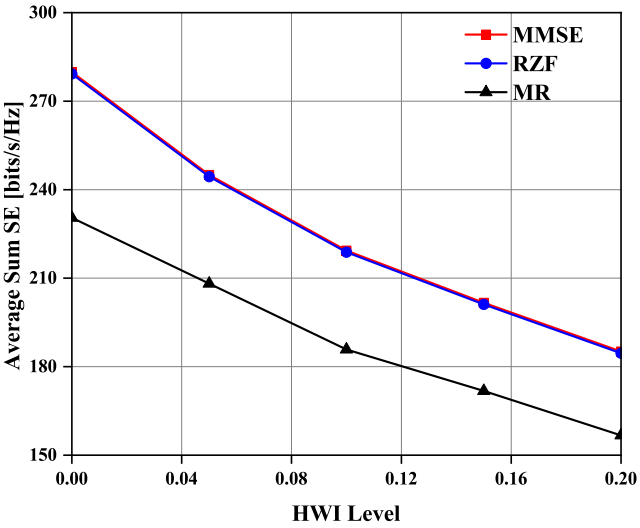

Figure 5. Average Sum SE against UE HWI factor

From Figure 5, it is observed that MMSE and RZF exhibit very close performance, with MMSE slightly outperforming RZF, particularly at higher SE values. Both MMSE and RZF curves are steeper than that of MR, indicating that their SE values are more concentrated around a central range, reflecting more predictable and consistent performance. In contrast, the MR combining scheme displays a wider spread in the CDF, signifying higher variability and less reliable SE across different realizations of the channel.

To validate the performance of combining schemes using the stochastic model with HWI, the Average Sum Spectral Efficiency (SE) at different HWI levels for different receiver combining schemes was investigated as shown in Figure 5. As expected, the Average Sum SE decreases monotonically with increasing HWI level for all schemes, confirming the detrimental effect of hardware impairments at the UE. Importantly, the figure shows that the rate of degradation in SE is nearly identical for both MMSE and RZF across all HWI levels considered. MMSE consistently maintains a slight advantage over RZF due to its superior interference mitigation capabilities, albeit at a higher computational cost. The

MR scheme, however, performs significantly worse across the board, emphasizing its susceptibility to distortion effects introduced by HWI.

Finally, in Figure 6, the Average Sum SE is plotted against the number of active UEs for the three combining schemes, both with and without hardware impairments. This figure vividly highlights the performance loss attributable to HWIs, particularly as the number of UEs increases. A notable observation from the figure is that MMSE and RZF without impairments outperform MR even with ideal conditions when the number of UEs exceeds approximately K = 48. This reinforces the finding that MR should be avoided in dense multi-user scenarios. Furthermore, it demonstrates that MMSE and RZF remain more robust even in the presence of hardware distortions from many users, while MR' s efficiency continues to degrade substantially as more users are introduced.

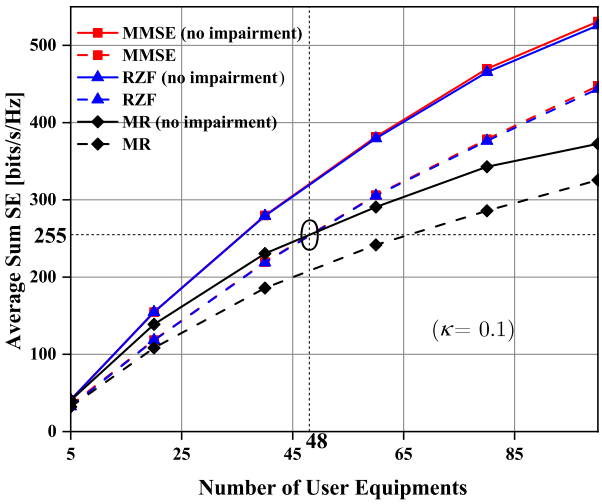

Figure 6. Average Sum SE when varying number of active UEs

For comparison purposes, Table 3 shows the average SE per user from different related works considering MMSE combining under various network scenarios. The values show a consistent trend in the achievable SE per UE when all factors are treated equally and HWI is introduced into the systems. This proves that further research and practical use of the CF-mMIMO system should take into account HWI from UE to correctly predict and assess network performance. Remarkably, it was anticipated that the ULA would support the body of current literature by improving SE performance as the number of antenna elements increased. Nonetheless, the correlated Rayleigh channel's performance was somewhat worse than that of the stochastic channel with ULA. This is because the channel vector now includes spatial surrounds. Considering the hypothetical scenario of generating the channel vector in an ideal (non-spatial) environment, we validate this. As a result, the SE increased by 55.62%. Thus, it is evident that one crucial factor in CF-mMIMO is that the spatial context in channel modeling should not be underestimated. Moreover, for a cell-free stochastic mMIMO with significant HWIs, advanced processing techniques (such as MMSE) are essential to maintain acceptable performance, even though MR might be more robust, but at the cost of lower overall efficiency.

Table 3. Per-user SE comparison in different network scenarios in the presence of HWI

Ref.	Channel Model	Spatial Environment	Network Scenario	Hardware Impairment $\kappa_t(UE), \kappa_r$(AP)	Link Analysis	Combining Scheme	Average Per-user Uplink SE (bit/s/Hz)
[4]	Uncorrelated Rayleigh	✗	L=200, K=10, N=1	0.02, 0.0	Uplink, Downlink	-	3.6
[12]	Correlated Rayleigh	✗	L=200, K=40, N=3	0.1, 0.3	Uplink	MMSE PMMSE MR	4.5 3.8 2.5
[22]	Correlated Rayleigh	✗	L=-, K=10, N=5	0.0, 0.0	Downlink	MR	2.6
[14]	Joint-Correlated Rayleigh	✗	L=40, K=10, N=4	0.1, 0.0	Uplink	MMSE PMMSE MR	3.3 2.8 2
[28]	Correlated Rayleigh	✗	L=100, K=40, N=4	0.1, 0.0	Uplink	MMSE RZF MR	5.75 5.5 3.38
Proposedwork	Stochastic Geometry	✓	L=100, K=40, N=4	0.1, 0.0	Uplink	MMSE RZF MR	5.5 5.4 4.5

5. Conclusion

In this paper, we investigated the impact of User Equipment (UE) Hardware Impairments (HWIs) on the performance of CF-mMIMO networks, with a specific focus on the degradation of uplink Spectral Efficiency (SE). The study employed a geometry-based stochastic channel model incorporating delay profile, path loss, and angle of arrival to evaluate the network and hardware distortion effects comprehensively.

Monte Carlo simulations revealed that while MMSE occasionally outperforms RZF by a small margin, this comes at the cost of higher computational complexity due to matrix operations. Quantitatively, we observed that both MMSE and RZF experience a 55.62% increase in SE when comparing the stochastic spatial channel to an idealized non-spatial scenario, highlighting the significant influence of spatial modeling on achievable rates. Additionally, the rate of degradation in SE for MMSE and RZF was found to be nearly identical in the stochastic model, whereas MR consistently showed lower efficiency and greater vulnerability to HWIs.

Among the three combining schemes analyzed, RZF provides a practical trade-off between computational complexity and SE performance, particularly in systems with a large number of users. MR, however, should be avoided in noisy or dense environments due to its inability to account for noise variance. Furthermore, our results emphasized that SE consistently degrades as the severity of hardware impairments increases at the user equipment side.

With the established link between improved channel estimation and achievable rates, an important direction for future research is to explore the integration of advanced machine learning techniques for channel estimation. Such approaches may further mitigate the effects of HWI, potentially rendering their impact negligible in next-generation wireless systems.

Conflict of interest

The authors declare no competing financial interest.

References

[1] T. L. Marzetta, "Noncooperative cellular wireless with unlimited numbers of base station antennas," *IEEE Transactions on Wireless Communications*, vol. 9, no. 11, pp. 3590-3600, 2010.

[2] H. C. Ngo, A. Ashikhmin, H. Yang, E. G. Larsson, and T. L. Marzetta, "Cell-free massive MIMO versus small cells," *IEEE Transactions on Wireless Communications*, vol. 16, no. 3, pp. 1834-1850, 2017.

[3] E. Bjornson, and L. Sanguinetti, "Making cell-free massive MIMO competitive with MMSE processing and centralized implementation," *IEEE Transactions on Wireless Communications*, vol. 19, no. 1, pp. 77-99, 2019.

[4] J. Zhang, Y. Wei, E. Björnson, Y. Han, and S. Jin, "Performance analysis and power control of cell-free massive MIMO systems with hardware impairments," *IEEE Access*, vol. 6, pp. 55302-55314, 2018.

[5] U. Gustavsson, C. Sanchéz-Perez, T. Eriksson, F. Athley, G. Durisi, P. Landin, et al., "On the impact of hardware impairments on massive MIMO," in *2014 IEEE Globecom Workshops (GC Wkshps)*, IEEE, pp. 294-300, 2014.

[6] X. Zhang, M. Matthaiou, E. Björnson, M. Coldrey, and M. Debbah, "On the MIMO capacity with residual transceiver hardware impairments," in *2014 IEEE International Conference on Communications (ICC)*, IEEE, pp. 5299-5305, 2014.

[7] E. Björnson, J. Hoydis, M. Kountouris, and M. Debbah, "Massive MIMO systems with non-ideal hardware: Energy efficiency, estimation, and capacity limits," *IEEE Transactions on Information Theory*, vol. 60, no. 11, pp. 7112-7139, 2014.

[8] S. Jacobsson, U. Gustavsson, G. Durisi, and C. Studer, "Massive MU-MIMO-OFDM uplink with hardware impairments: Modeling and analysis," In Proc. 52nd Asilomar Conference on Signals, Systems, and Computers, Pacific Grove, CA, USA, Oct. 28-31, 2018, pp. 1829-1835.

[9] E. Björnson, L. Sanguinetti, and J. Hoydis, "Hardware distortion correlation has negligible impact on UL massive MIMO spectral efficiency," *IEEE Transactions on Communications*, vol. 67, no. 2, pp. 1085-1098, 2018.

[10] J. Zheng, J. Zhang, L. Zhang, X. Zhang, and B. Ai, "Efficient receiver design for uplink cell-free massive MIMO with hardware impairments," *IEEE Transactions on Vehicular Technology*, vol. 69, no. 4, pp. 4537-4541, 2020.

[11] H. Masoumi, and M. J. Emadi, "Performance analysis of cell-free massive MIMO system with limited fronthaul capacity and hardware impairments," *IEEE Transactions on Wireless Communications*, vol. 19, no. 2, pp. 1038-1053, 2019.

[12] A. K. Papazafeiropoulos, E. Björnson, P. Kourtessis, S. Chatzinotas, and J. M. Senior, "Scalable cell-free massive MIMO systems with hardware impairments," In Proc. IEEE 31st Annual International Symposium on Personal, Indoor and Mobile Radio Communications, London, UK, Aug. 31-Sep. 3, 2020, pp. 1-7.

[13] A. Papazafeiropoulos, E. Björnson, P. Kourtessis, S. Chatzinotas, and J. M. Senior, "Scalable cell-free massive MIMO systems: impact of hardware impairments," *IEEE Transactions on Vehicular Technology*, vol. 70, no. 10, pp. 9701-9715, 2021.

[14] M. Xie, X. Yu, Y. Rui, K. Wang, X. Dang, and J. Zhang, "Performance analysis for user-centric cell-free massive MIMO systems with hardware impairments and multi-antenna users," *IEEE Transactions on Wireless Communications*, vol. 23, no. 2, pp. 1243-1259, 2023.

[15] X. Hu, C. Zhong, X. Chen, W. Xu, H. Lin, and Z. Zhang, "Cell-free massive MIMO systems with low resolution ADCs," *IEEE Transactions on Communications*, vol. 67, no. 10, pp. 6844-6857, 2019.

[16] N. Li and P. Fan, "Spatially correlated cell-free massive MIMO network with centralized operation and low-resolution ADCs," In Proc. IEEE 98th Vehicular Technology Conference, Hong Kong, China, Oct. 10-13, 2023, pp. 1-6.

[17] Y. Zhang, M. Zhou, Y. Cheng, L. Yang, and H. Zhu, "RF impairments and low-resolution ADCs for nonideal uplink cell-free massive MIMO systems," *IEEE Systems Journal*, vol. 15, no. 2, pp. 2519-2530, 2020.

[18] J. Zhang, J. Zhang, and B. Ai, "Cell-free massive MIMO with low-resolution ADCs over spatially correlated channels," In Proc. IEEE International Conference on Communications, Dublin, Ireland, Jun. 7-11, 2020, pp. 1-7.

[19] Y. Zhang, Q. Zhang, H. Hu, L. Yang, and H. Zhu, "Cell-free massive MIMO systems with non-ideal hardware: Phase drifts and distortion noise," *IEEE Transactions on Vehicular Technology*, vol. 70, no. 11, pp. 11604-11618, 2021.

[20] M. Xie, X. Yu, J. Xu, and X. Dang, "Low-complexity channel estimation scheme for cell-free massive MIMO with hardware impairment," In Proc. IEEE Global Communications Conference, Rio de Janeiro, Brazil, Dec. 4-8, 2022, pp. 711-716.

[21] J. Zhang, Y. Wei, E. Björnson, Y. Han, and X. Li, "Spectral and energy efficiency of cell-free massive MIMO systems with hardware impairments," In Proc. 9th International Conference on Wireless Communications and Signal Processing, Nanjing, China, Oct. 11-13, 2017, pp. 1-6.

[22] A. Papazafeiropoulos, P. Kourtessis, M. Di Renzo, S. Chatzinotas, and J. M. Senior, "Performance analysis of cell-free massive MIMO systems: A stochastic geometry approach," *IEEE Transactions on Vehicular Technology*, vol. 69, no. 4, pp. 3523-3537, 2020.

[23] H. Haritha, D. N. Amudala, R. Budhiraja, and A. K. Chaturvedi, "Superimposed versus regular pilots for hardware impaired Rician-faded cell-free massive MIMO systems," *IEEE Transactions on Communications*, 2024.

[24] E. Björnson, L. Sanguinetti, and M. Kountouris, "Deploying dense networks for maximal energy efficiency: Small cells meet massive MIMO," *IEEE Journal on Selected Areas in Communications*, vol. 34, no. 4, pp. 832-847, 2016.

[25] B. Vaishnavi and K. K. Sharma, "Evaluation of the effect of 5G hardware impairments on achieving high energy efficiency," In Proc. Journal of Physics: Conference Series, 2022, vol. 2327, no. 1, p. 012047.

[26] J. Zhu, D. W. K. Ng, N. Wang, R. Schober, and V. K. Bhargava, "Analysis and design of secure massive MIMO systems in the presence of hardware impairments," *IEEE Transactions on Wireless Communications*, vol. 16, no. 3, pp. 2001-2016, 2017.

[27] X. Zhang, D. Guo, K. An, and B. Zhang, "Secure communications over cell-free massive MIMO networks with hardware impairments," *IEEE Systems Journal*, vol. 14, no. 2, pp. 1909-1920, 2019.

[28] N. Li and P. Fan, "Impact of UE hardware impairments on uplink spectral efficiency of cell-free massive MIMO network," In Proc. IEEE Wireless Communications and Networking Conference, Glasgow, UK, Mar. 26-29, 2023, pp. 1-6.

[29] Y. Zhang, H. Zhao, W. Xia, W. Xu, C. Tang, and H. Zhu, "How much does reconfigurable intelligent surface improve cell-free massive MIMO uplink with hardware impairments?" *IEEE Transactions on Communications*, 2023.

[30] E. Bjornson, M. Matthaiou, and M. Debbah, "A new look at dual-hop relaying: Performance limits with hardware impairments," *IEEE Transactions on Communications*, vol. 61, no. 11, pp. 4512-4525, 2013.